Diffusion Tensor Imaging of the Superior Thalamic Radiation and Cerebrospinal Fluid Distribution in Idiopathic Normal Pressure Hydrocephalus

Kyan Younes, Khader M. Hasan, Arash Kamali, Christine E. McGough, Zafer Keser, Omar Hasan, Tomas Melicher, Larry A. Kramer, Paul E. Schulz, the Alzheimer's Disease Neuroimaging Initiative Researchers

From the Department of Neurology, McGovern Medical School, University of Texas Health Science Center (UTHSC), Houston, TX (KY, CEM, ZK, OH, PES); Department of Diagnostic and Interventional Imaging, McGovern Medical School, University of Texas Health Science Center (UTHSC), Houston, TX (KMH, AK, LAK); and Department of Psychiatry, McGovern Medical School, University of Texas Health Science Center (UTHSC), Houston, TX (TM).

ABSTRACT

BACKGROUND AND PURPOSE: **Ventricular enlargement in elderly raises a challenging differential diagnosis to physicians. While Alzheimer's disease is the most common form of dementia, idiopathic normal pressure hydrocephalus (iNPH) constitutes a potentially reversible syndrome. iNPH has a unique pathophysiology pertaining to cerebrospinal fluid (CSF) dynamics and periventricular white matter. We aimed to determine the effects of iNPH on periventricular white matter bundles and to further characterize its ventricular and sulcal CSF distribution by using diffusion tensor tractography (DTT) and CSF volumetrics on high resolution T1-weighted magnetic resonance imaging data.**

METHODS: **Deterministic DTT and validated volumetric parcellation were performed on 20 healthy elderly, 13 Alzheimer's disease (AD), and 9 iNPH patients. The superior thalamic radiation, corticospinal tract, and dentatorubrothalamic tract were traced and quantified using DTI studio software. Cloud-based volumetric parcellation was also performed on 138 healthy subjects across the lifespan, 13 AD, and 9 iNPH-patients. Ventricular and sulcal CSF volumes in the three groups were compared.**

RESULTS: **Combining increased mean diffusivity of the superior thalamic radiation with ventricular volume resulted in clear separation of iNPH from the AD and age-matched healthy subject groups. Additionally, ventricular to sulcal CSF ratio, utilizing fully automated methods, was significantly greater in the iNPH patients compared to AD and healthy age-matched controls.**

CONCLUSIONS: **Combined microstructural (DTT) and macrostructural (ventricular volume) changes is a promising radiological approach in studying ventriculomegaly. Automated estimation of the disproportionate ventricular and sulcal CSF ratio in patients presenting with ventriculomegaly may be important as radiologic markers in differentiating iNPH from other causes of ventriculomegaly.**

Keywords: dentatorubrothalamic tract, diffusion tensor tractography, normal pressure hydrocephalus, superior thalamic radiation, ventricular volume.

Acceptance: Received May 31, 2018, and in revised form October 25, 2018. Accepted for publication October 26, 2018.

Correspondence: Address correspondence to Khader M. Hasan, Department of Diagnostic and Interventional Radiology, McGovern Medical School, University of Texas, 6431 Fannin St. Houston, TX 77030. E-mail: Khader.M.Hasan@uth.tmc.edu.

Acknowledgements: This study was funded in part by DUNN research foundation to KMH. We wish to thank Vipul Kumar Patel for helping in data acquisition. The Alzheimer's disease Neuroimaging Initiative Data used in preparation of this article were obtained from the Alzheimer's disease Neuroimaging Initiative (ADNI) database (adni.loni.usc.edu). As such, the investigators within the ADNI contributed to the design and implementation of ADNI and/or provided data but did not participate in analysis or writing of this report. A complete listing of ADNI investigators can be found at: http://adni.loni.usc.edu/wp-content/uploads/how_to_apply/ADNI_Acknowledgement_List.pdf.

Conflicts of Interest: The authors have no potential conflict of interest to disclose.

J Neuroimaging 2019;29:242-251.
DOI: 10.1111/jon.12581

Introduction

Ventriculomegaly is a challenging neuroimaging finding neurologists frequently face in the aging population.[1] Hydrocephalus is a general term that indicates accumulation of cerebrospinal fluid (CSF) in the ventricular system due to imbalance in the production, drainage, or reabsorption of CSF resulting in dilation of the cerebral ventricles.[2] It is classified into obstructive versus nonobstructive and communicating versus noncommunicating hydrocephalus based on the presence or absence of an identifiable near blockage of the CSF flow and at the location of this near blockage when present, respectively.[2] If the increase in the ventricular volume (VV) is due to cerebral atrophy secondary to gray or white matter (WM) volume loss, it is called hydrocephalus ex vacuo.[1] Idiopathic normal pressure hydrocephalus (iNPH) is a form of chronic communicating hydrocephalus that results in a treatable syndrome characterized by the triad of gait impairment, progressive dementia, and urinary incontinence.[3,4] iNPH prevalence is estimated to be 21.9 of 100,000 and increases with age, with an incidence of approximately 5.5 of 100,000 per year.[5] Other neurodegenerative diseases, such as Alzheimer's, vascular dementia, and Parkinson's diseases, are also common in the same age population. Studies have shown coexistence of increased rate of Alzheimer's disease (AD) histopathology in patients with iNPH beyond what can be accounted for by chance alone.[6,7] Studies have shown decrease CSF production and turnover in both

AD and NPH.[8] It was postulated by Silverberg that failure of CSF production or increased CSF flow resistance might lead to either AD, iNPH, or AD–NPH depending on which pathological process predominates.[9] More recent data showed delayed clearance of the CSF from the entorhinal cortex in iNPH patients suggesting involvement of the glymphatic system in the pathophysiology of iNPH.[10–12] Understanding the underlying pathophysiology of iNPH carries an importance beyond iNPH itself, as it relates to the brain CSF hydrodynamics relationship and pertains to questions regarding aging and Alzheimer's disease pathophysiology.

According to both the International and the Japanese iNPH guidelines,[2,4] the diagnosis of iNPH is suspected based on the combination of clinical evaluation and neuroimaging and is confirmed based on the response to an invasive procedure such as CSF tap test or external CSF drain.[5] Therefore, the complexity of ventriculomegaly and particularly iNPH diagnosis and management appears to be multifactorial. Magnetic resonance imaging (MRI), especially diffusion tensor imaging (DTI), has shown to offer a useful in vivo surrogate biomarkers of WM changes in AD,[13,14] ventriculomegaly,[15] and iNPH.[16,17] Previous studies using deterministic and probabilistic DTI techniques revealed various profiles of DTI changes in different regions of the periventricular WM when compared to normal and disease controls.[16,17] A consensus is still not established for the most sensitive and specific DTI measurements in distinguishing ventriculomegaly in iNPH from other neurodegenerative diseases.

Neuroimaging noninvasive markers for iNPH are a critical need, we propose a new technique to differentiate NPH from healthy and disease controls using novel MRI-DTI targets. In this study, we provide quantitative DTI mapping of main WM pathways neighboring the lateral ventricular system. We analyzed the effect of iNPH on the superior thalamic radiation (STR) as it courses adjacent to the lateral wall of the lateral ventricle. The corticospinal tract (CST) and the dentatorubro thalamic tract (DRTT). Moreover, we investigated the volumetric changes of the ventricular and sulcal CSF in AD, iNPH, and healthy aging subjects across lifespan.

Methods

Subjects

We included 13 single-center Alzheimer's patients (7 females and 6 males, age range = 65–87 years, mean = 73 years, standard deviation = 6.9 years), 9 iNPH patients (5 females and 4 males, age range = 61–91 years, mean = 77.2 years, standard deviation = 8.6 years), and 20 normal healthy adults (11 females and 9 males, age range = 62–85 years, mean = 75 years, standard deviation = 7.1 years) in our analysis. Twenty healthy patients were the elderly subset of 138 patients subjects imaged across lifespan (57 males and 81 males, age range = 5–85 years, mean = 35.5 years, standard deviation = 20.4 years). The AD patient data were collected by the Alzheimer's Disease Neuroimaging Initiative (ADNI) database (adni.loni.usc.edu). The ADNI was launched in 2003 as a public–private partnership, led by Principal Investigator Michael W. Weiner, MD. The primary goal of ADNI has been to test whether serial MRI, positron emission tomography (PET), other biological markers, and clinical and neuropsychological assessment can be combined to measure the progression of mild cognitive impairment and early AD. For up-to-date information, see www.adni-info.org, full eligibility criteria for the ADNI are described in the ADNI2 procedures manual (Alzheimer's Disease Neuroimaging Initiative, 2008). The healthy group DTI was acquired from the International Neuroimaging Data Sharing Initiative (INDI) online database (https://fcon_1000.projects.nitrc.org/indi/pro/nki.html). Additional variables included subjects' age. This sample was provided by the Nathan Kline Institute (NKI, NY) as part of the "original NKI-Rockland sample." All necessary approvals and procedures for human subject studies were followed as required by ADNI and NKI. The iNPH patients were enrolled in the study following University of Texas Health Science Center at Houston Institutional Review Board approval and diagnosed with probable iNPH per the International iNPH guidelines.[4] The iNPH patients were followed by a dementia specialist over time and iNPH diagnoses confirmed with serial lumbar puncture tap test. All iNPH patients had Evans index >.3, calculated on the axial view by dividing the largest width of the frontal horns by the largest width of the skull.[16] Patients were medically stable at the time of the assessments. Three out of the nine patients had positive Disproportionately Enlarged Subarachnoid-space Hydrocephalus (DESH) sign on coronal cuts of their initial MRI.[5] Montreal Cognitive Assessment (MOCA) was done on the initial evaluation as a cognitive screen (see Table 1 for clinical characteristics and demographics of the iNPH patients).

MRI Data Acquisition

In regards to the iNPH subjects, whole-brain MRI data were acquired using a Philips 3.0 T Intera system with a SENSE parallel image receiving head coil with 15 channels (Philips Medical Systems, Best, Netherlands). The MRI protocol included (1) 3-dimensional (3D) fluid attenuated inversion recovery and 3D T2-weighted and 3D spoiled gradient echo (T1-weighed) data, field of view = 256 × 256 mm (isotropic voxel size = 1 mm); and (2). Diffusion-weighted data using a single-shot, spin-echo diffusion sensitized echo-planar imaging (EPI) sequence with the balanced Icosa21-encoding scheme,[18,19] a diffusion sensitization of $b = 1{,}000$ s/mm^2, and repetition times (TRs) and echo times (TEs) of 7,900 ms and 70 ms, respectively. EPI distortion artifacts and scan time were reduced by using a SENSE acceleration factor (R) or k-space under sampling equals to 2 (ie, $R = 2$).[19–21] The slice thickness was 3 mm with 48 axial slices covering the entire brain, foramen magnum to vertex, a square field of view (FOV) = 256 × 256 mm^2, and an image matrix of 256 × 256. The average number of nondiffusion-weighted or $b \sim 0$ magnitude image was 8. The total DTI acquisition time was approximately 7 min and resulted in signal-to-noise ratio (SNR)-independent DTI metric estimation.[22]

The healthy NKI group DTI images were acquired using a 3.0 T Siemens Trio scanner (Siemens Medical Systems, Erlangen, Germany) with a spin echo–EPI factor = 128, TE/TR = 91/10,000 ms, FOV = 256 mm, spatial resolution = 2.0 × 2.0 × 2.0 mm, 64 diffusion encoding gradients, b value = 1,000 s/mm^2, and 12 nondiffusion volumes. Further details about the study image acquisition protocol are available on the INDI website as provided above. These data have been made available to all researchers around the world for the purpose of discovery science and potentially for replication of results in different laboratories.

Table 1. Clinical Characteristics of Idiopathic Normal Pressure Hydrocephalus Patients

Patient	Age	Gender	MOCA	NPH Symptoms	Duration of Symptoms (Years)	DESH	Evans Index
iNPH1	91	Male	8	Cognitive and gait	3	(+)	.33
iNPH2	71	Female	22	Cognitive, gait, and incontinence	1	(−)	.36
iNPH3	78	Female	29	Cognitive, gait change, and incontinence	2	(−)	.35
iNPH4	72	Female	21	Cognitive, gait change, and incontinence	2	(−)	.31
iNPH5	61	Male	27	Cognitive, gait change, and incontinence	2	(−)	.34
iNPH6	80	Male	20	Cognitive, gait,	2	(+)	.38
iNPH7	77	Male	18	Cognitive, gait,	1	(+)	.37
iNPH8	85	Female	15	Cognitive, gait, and incontinence	2	(−)	.45
iNPH9	80	Female	29	Cognitive, gait change	1	(−)	.30

DESH = disproportionately enlarged subarachnoid-space hydrocephalus; iNPH = idiopathic normal pressure hydrocephalus; MOCA = Montreal Cognitive Assessment.

The ADNI cohort MRI, standard MRI, dMRI, and clinical data were downloaded from the publicly available ADNI database (www.loni.usc.edu/ADNI). Whole-brain MRI data were acquired using a Siemens Verio 3T system–gradient coils capable of 45 mT/m and 200 T/m/s slew rate–with a 32-channel phased-array head-coil. Diffusion volumes were acquired using a standard twice-refocused, single-shot EPI pulse sequence: TR/TE = 56/7,200 ms; matrix = 116 × 116; 80 contiguous slices; voxel size: 2 × 2 ×2 mm^3; number of $b \sim 0$ volumes = 7; b factor = 1,000 at 48 uniformly distributed diffusion encoding orientations, bandwidth of Hz/pixel, and echo spacing of .68 ms. In order to assure the quality of DTI data, regional and global gray matter, white matter and CSF fractional anisotropy (FA), and mean diffusivity (MD) histograms were evaluated. Voxel size, b factor calibration and signal-to-noise ratio on $b0$, and diffusion-weighted images were deemed acceptable on all protocols to enable DTI-based tissue segmentation using FA and MD (see Fig 1). In an attempt to prevent type I error, we computed false discovery rate (FDR) by using the Benjamini–Hochberg method as described in detail elsewhere to adjust for multiple comparisons.[23] We calculated adjusted P values derived from P values of all the correlation analyses between diffusion tensor parameters correlation and lateral ventricles in subjects with iNPH, AD, and healthy subjects, and comparison analyses of ventricular and sulcal subarachnoid CSF among the aforementioned subject groups to determine which values from the data remain significant at an FDR of .10.

Tissue Segmentation and Parcellation Using T1-Weighted Data

After inspection for quality and preparation that included reformatting, the T1-weighted brain data were fully segmented using the MRI Cloud (https://braingps.mricloud.org/) online software package.[24] VVs were obtained based on the T1-weighted data segmentation. Right and left lateral ventricles were segmented to fontal, body, atrium, occipital, and inferior compartments. The third and fourth VVs were also obtained. Sulcal CSF was segmented to left and right frontal, central, sylvian frontal, sylvian temporal, sylvian parietal, parietal, cingulum, occipital, and temporal. All volumes reported in this study were adjusted to intracranial volume (ICV). Sylvian CSF was studied as a part of the total sulcal CSF, as well as a separate portion of the sulcal CSF by subtracting the sylvian sulcal CSF volume from the total sulcal CSF volume.

Diffusion Tensor Tractography

After DWI data preparation that included visual inspection, registration, and averaging,[22] compact fiber tracking was performed using DTI Studio software (John Hopkins University, Baltimore, MD; https://cmrm.med.jhmi.edu). Fiber tracking was based by the Fiber Assignment by Continuous Tracking algorithm with a FA threshold of .15 and angle threshold of 70°. Brute-force fiber tractography and multiple region of interest techniques were utilized to track the pathways of interest. Once a fiber tract was reconstructed, the entire trajectory was verified on a slice-by-slice basis to ensure consistency with established anatomical landmarks.[25] All tracts were visually inspected for quality assurance in all the subjects of the three different groups. The mean FA and MD were calculated from the individual values obtained from all the voxels that contained the fiber tract. The transverse and axial diffusivities were calculated as described elsewhere.[22] All the above described pathways were separated with minor modifications to the traditional DTT methods described in the past.[25] The diffusion metrics were quantified for each of the individual tracts bilaterally.

Anatomical Landmarks and DTI Reconstruction

Superior Thalamic Radiation (STR)

WM fiber bundles that reciprocally connect the thalamus and the cortex constitute the thalamic radiations. The thalamic radiations are grouped into four subradiations designated as the thalamic peduncles. The superior or centroparietal peduncle connects the pre- and postcentral gyri and adjacent portions of the frontal and parietal lobes with the ventral thalamic nuclei. The STR constitutes the medial part of the superior corona radiata and runs medial to the CST.[26] To reconstruct the STR (see Fig 2), the entire 3D volume of the thalamus was defined as the first ROI. The second ROI was placed over the entire hemisphere within a transverse section above the corpus callosum.[25]

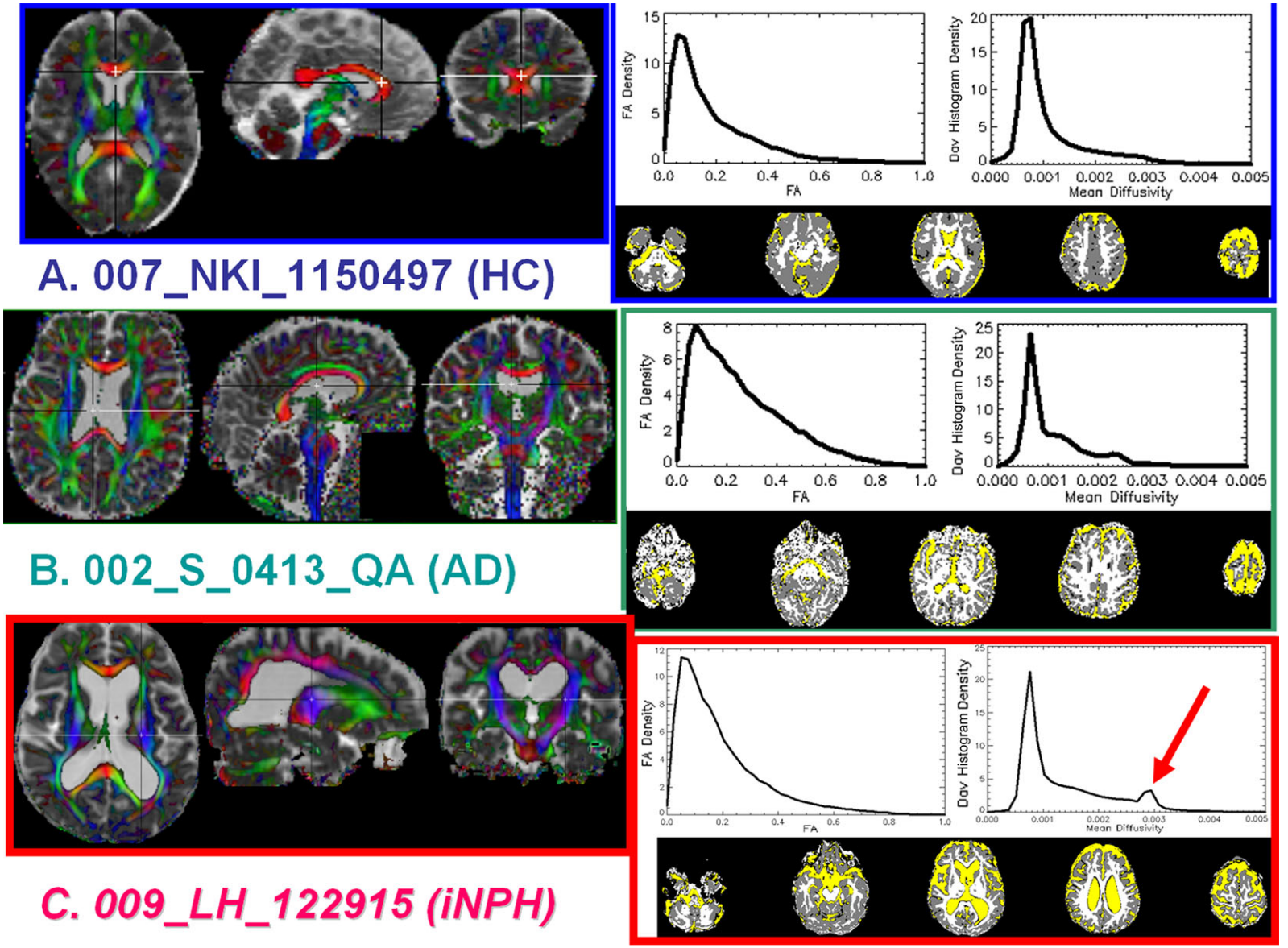

Fig 1. Quality assurance to assure diffusion tensor imaging data fidelity across scanners. (A) Regional and global gray matter, white matter, and cerebrospinal fluid segmentation using fractional anisotropy and mean diffusivity thresholds determined by (B) histogram analysis from three subjects: healthy elderly, Alzheimer's disease (AD), and idiopathic normal pressure hydrocephalus (iNPH) patients. (C) The principal Eigenvector modulated by fractional anisotropy (FA) and fused with mean diffusivity map is shown in 3D. Arrow: CSF peak on mean diffusivity (MD) histogram of the iNPH case. Tissue segmentation thresholds (white matter = FA > .2 and MD < .0017 mm^2/s; CSF = FA < .2 and MD > .0025; gray matter = FA < .2 and MD < .0017 mm^2/s).
HC = healthy control; DAV = diffusion average.

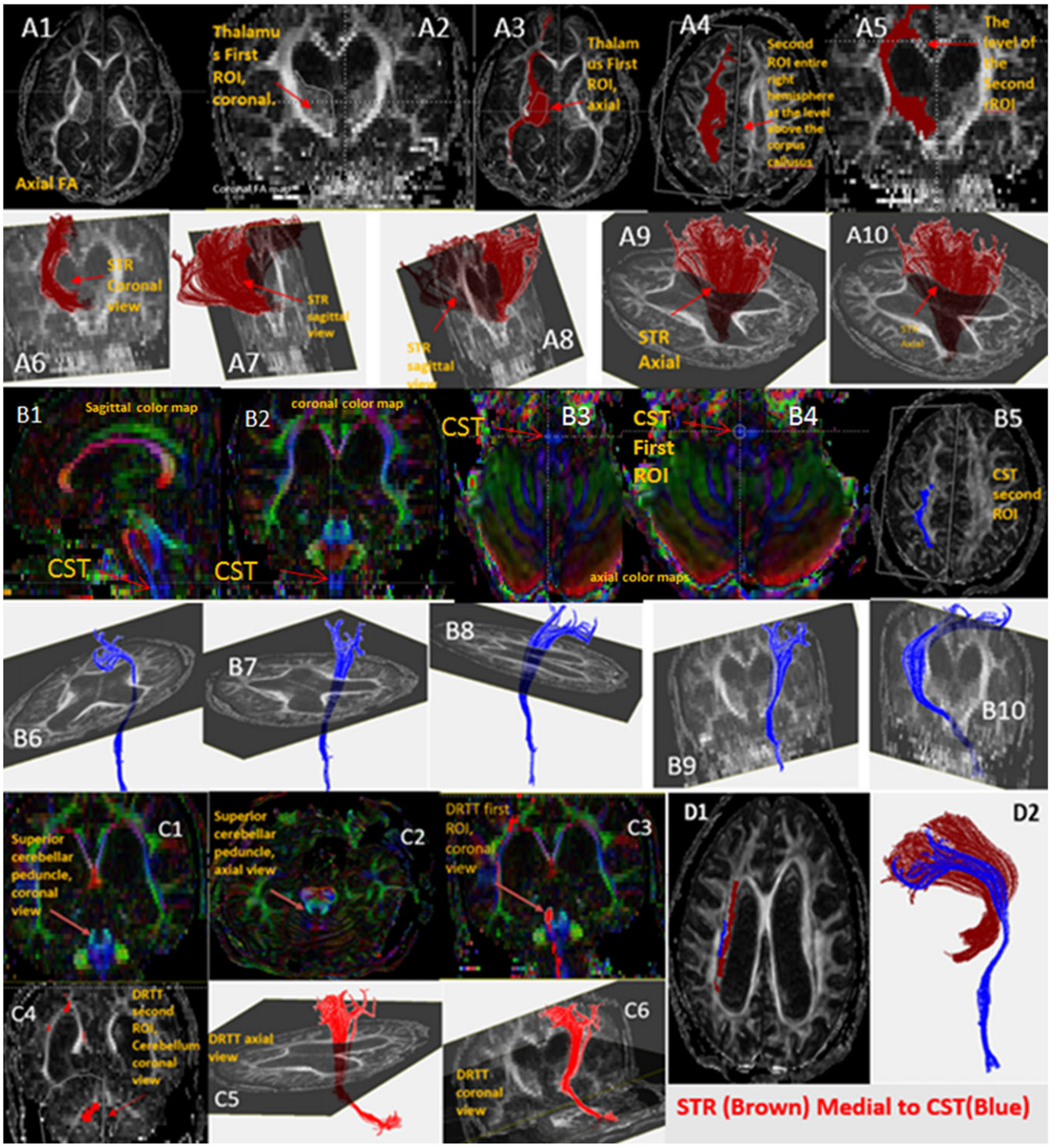

Fig 2. Anatomical landmarks and diffusion tensor imaging reconstruction. (A) Represents the superior thalamic tract (STR) reconstruction, the entire 3D volume of the thalamus was defined as the first region of interest (ROI) (A2-A3) and the second ROI was placed over the entire ipsilateral hemisphere within a transverse section above the corpus callosum (A4). (B) Represents the corticospinal tract reconstruction (CST), the first ROI is placed on the color map over the anterior cerebral peduncle on the level of mid pons as illustrated in (B4). The second ROI is placed ipsilateral over the motor cortex as shown in (B5). (C) Represents the dentatorubrothalamic tract, the first ROI is seeded over the superior cerebellar peduncle in the coronal view (C1) and second ROI in the ipsilateral cerebellar hemisphere over the ipsilateral cerebellar hemisphere at the level of the dentate nucleus (C4). (D) Represents the spatial relationship of the superior thalamic tract and the corticospinal tract.

Corticospinal Tract (CST)

The CST originates from the precentral motor cortex and descends through the corona radiata and posterior one-third portion of the posterior limb of internal capsule (pLIC) and the cerebral peduncle to the level of the pons and caudally to the medulla and spinal cord[26] (Fig 2B-B10). The first ROI is placed on the color map over the anterior medulla as illustrated in Fig 2B4. The second ROI is placed ipsilateral over the motor cortex as shown in Fig 2B5. Contaminant cortico–ponto–

cerebellar fibers are cleaned by careful slice-by-slice visual inspection.

Dentatorubrothalamic Tract (DRTT)

The main gray matter constituent of DRTT in the cerebellum is the dentate nuclei which have a clear contrast enhancement in the DWI nondiffusion *b*0 image because of the iron content in adults.[18] Thus to reconstruct DRTT (see Fig 2C1-6), the first ROI is seeded in the coronal section of the color map over the superior cerebellar peduncle (Fig 2C1,2) and second ROI in the ipsilateral cerebellar hemisphere at the level of the dentate nucleus (Fig 2C4).

Statistical Analyses

The VVs, fractional anisotropy (FA), mean diffusivity (MD), axial diffusivity (AD), and radial diffusivity (RD) on STR, CST and DRTT in the AD, NKI and iNPH cohorts were examined individually using unpaired *t*-test. The relation between VV and measured FA, MD, and transverse and axial diffusivities were examined using Spearman correlation analysis as our data could not assure normal distribution for all the variables likely due to small sample size. We used normalized volumetric measures scaled for each subject by the individual estimated ICV. Statistical analyses and generation of scatter plots were performed using SPSS Statistics 24.0-IBM software (Armonk, New York) and the statistical toolbox in MATLAB (Version 6.1; The MathWorks Inc., Natick, MA). Statistical significance was defined if $P < .05$.

Results

Micro- and Macrostructural DTI and Volumetry Correlations

The STR, CST, and DRTT were reconstructed on 13 AD, 9 iNPH patients (Fig 3) and 20 age-matched healthy elderly. DTI findings were tested in correlation to the total VV parentage. In the iNPH patients, a positive correlation was found between the axial diffusivity of the CST and the lateral VV, this was statistically significant on the left and marginally significant on the right. Similarly, the axial diffusivity of the STR was statistically significant on the left ($r = .750$, P value $= .02$; FDR corrected P value $= .08$), but not significant on the right. Finally, DRTT AD was marginally significant on the left and not significant on the right (see Table 2). In the AD patients, left STR FA correlation with the lateral ventricular percentage was statistically significant (FDR corrected P value $= .05$), but not on the right (STR MD, AD, or RD correlations with the lateral ventricle were not statistically significant). DRTT FA was statistically significant on the left, but not on the right DRTT. AD was statistically significant on the left but not on the right. In the 20 age-matched healthy elderly, axial and radial diffusivity changes in both CST and STR had a positive statistically significant correlation with the lateral VV. STR mean and axial diffusivities correlation were statistically significant bilaterally. Right STR AD did not survive FDR correction and also DRTT AD on the left did not survive FDR correction (see Table 2). Figure 4 shows that while the separation of AD from healthy elderly was driven solely by the increased VV, the separation of iNPH group from the other two groups was driven not only by the ventricular size but also by the accompanying increase in the tract's MD.

Ventricular and Sulcal Subarachnoid CSF Volumes

Ventricular CSF volumes (vCSFVs) and the sulcal subarachnoid CSF volumes (sCSFVs) were parcellated using the fully automated online MRI-cloud software packet for the AD, iNPH, and healthy subjects. Sylvian CSF was studied as a part of the total sulcal CSF, as well as a separate portion of the sulcal CSF as mentioned above. In the healthy group, the sCSFV was universally higher than the vCSF across lifespan. Both sCSF and vCSF increased with age and sCSF continued to be more than vCSF in the age-matched subgroup of the healthy subjects (see Fig 5). Data were illustrated in these two figures for the purpose of better visualization.

In the iNPH group, the increase in vCSFV was not associated with proportionate increase in the sCSFV, leading to vCSFV that is not significantly different from the sCSFV.

The vCSFV and sCSFV in the iNPH group were not significantly different. There was no significant difference in the sCSF between iNPH and age-matched healthy or AD sCSFV groups. Both ventricular and sulcal volumes were corrected for the ICV (see Table 3).

Total VV in the iNPH group was significantly higher than the AD and healthy elderly (HE) groups (P values $= .001$ (.01) and .001 (.01), respectively).

Sylvian CSF volume percentage in iNPH group was significantly higher than AD and HE groups (P values $= .043$ (FDR corrected P value $= .15$) and .002 (FDR corrected P value $= .011$), respectively). Sylvian CSF volume in AD group was significantly higher than the HE group (P value $= .001$) (FDR corrected P value $= .01$). Total sulcal CSF and sulcal CSF minus sylvian CSF volumes were not significantly different between iNPH and AD group (P values $= .46$ (FDR corrected P value $= .71$) and .232 (FDR corrected P value $= .39$), respectively). Total sulcal CSF and sulcal CSF minus sylvian CSF in iNPH group were significantly higher than the HE group (P value $= .003$ (FDR corrected P value $= .022$) and .044 (FDR corrected P value $= .15$), respectively). Total sulcal CSF and sulcal CSF minus Sylvian CSF in AD group were significantly higher than HE group (P value $= .001$ (FDR corrected P value $= .01$) and .001 (FDR corrected P value $= .01$), respectively).

Discussion

Our study demonstrates the feasibility and utility of deterministic fiber tractography analysis of the periventricular WM disease in iNPH. The STR, for the first time in iNPH patients, was traced and evaluated using the methods and protocols discussed above. The STR forms the most medial part of the superior corona radiata and runs medial to the CST.[26] We hypothesized that the STR will be affected by iNPH ventriculomegaly given its anatomical proximity to and its pattern of spread around the lateral ventricle wall (see STR tracking in Fig 2). In this study, we attempt to combine the dynamic interplay between the microstructural changes in the periventricular WM with the macrostructural characteristics of ventriculomegaly in iNPH. By combining these two measures we demonstrate the feasibility of differentiating the groups of interest based on two-dimension vector representation of pathology (see Fig 4). Combining both the VV and STR MD led to group separation of iNPH, AD, and HE. This demonstrates that while the separation of AD from healthy elderly was driven solely by the increased VV, the separation of iNPH group from

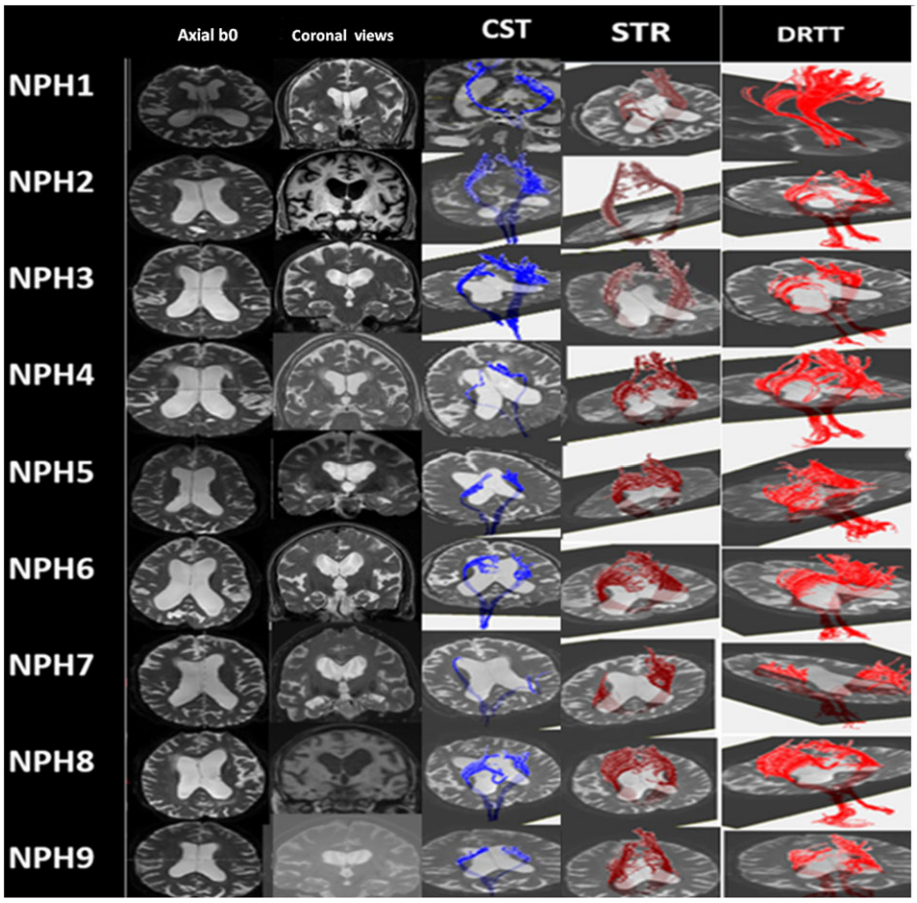

Fig 3. Axial and coronal MRI views of the idiopathic normal pressure hydrocephalus cases showing the ventriculomegaly. Diffusion tensor tractography of the corticospinal tract, superior thalamic tract, and dentatorubrothalamic tract.
CST = corticospinal tract; NPH = normal pressure hydrocephalus; STR = superior thalamic radiation; DRTT = dentatorubrothalamic tract.

the other two groups was driven not only by the ventricular size but also by the accompanying increase in the tract's MD. The increase in VV was associated with increase in the MD, driven mainly by changes in the axial diffusivity. The relationship between MD and VV describes a 2-dimensional marker of iNPH that separates it clearly from the AD and age-matched healthy controls. This radiographic marker may reflect the in vivo interaction between ventriculomegaly and WM changes. Combining volumetric and DTI led to an increase in the difference between the groups capturing the changes in iNPH by addressing both the increased ventricular size, as well as the increased diffusivity in the periventricular WM.

Several quantitative and volumetric techniques have been proposed and used in the diagnoses of iNPH. Evan's index and DESH are already being used as a part of the diagnostic criteria of iNPH.[4,5] More automatic techniques have been studied; Tsunoda and coauthors measured the VV over the ICV ratio in iNPH, cerebrovascular disease patient, and HE and found that most iNPH had a VV/ICV ratio above 30% while none of the control subjects had a ratio above 30%.[19] VV reported as 49.9 ± 25.3 mL in AD using semiautomatic segmentation software.[14] One of the radiological signs of iNPH is hydrocephalus out of proportion to the cortical atrophy.[20] We adopted a novel validated and fully automated quantitative volumetric approach to calculate the ventricular and sulcal CSF components. By analyzing the total sulcal and the

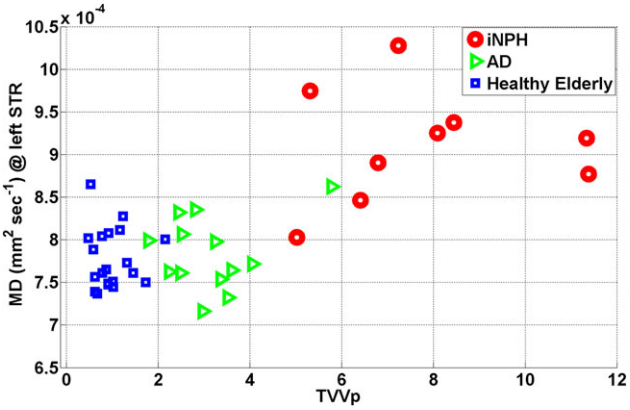

Fig 4. Superior thalamic radiation (STR) mean diffusivity (MD) correlation with the ventricle volume (VV) in healthy elderly, Alzheimer's disease (AD), and idiopathic normal pressure hydrocephalus (iNPH) patients. Clear clustering of the healthy (yellow pentagons), the Alzheimer's (green squares), the iNPH patients (blue circles) based on mean diffusivity correlation of the STR with the VV. The VV is corrected to the intracranial volume.
TVVp = total ventricle volume percentage adjusted to the intracranial volume.

sylvian sulcal CSF, we found that the mean sulcal CSF was greater in the AD cohort than the iNPH, however, the difference did not reach statistical significance. This might be

Table 2. Diffusion Tensor Parameters Correlation with Lateral Ventricles

		iNPH		Alzheimer's		Healthy Controls	
FA_CST	*r*	.467	.583	.5	.346	−.406	−.174
	P	.205	.099	.082	.247	.076	.462
	corr *P*	.386	.236	.214	.417	.205	.693
MD_CST	*r*	−.15	.283	.363	.0001	.765	.644
	P	.7	.46	.223	1	.0001*	.462
	corr *P*	.872	.703	.4014	1	.0027**	.6804
RD_CST	*r*	−.217	−.217	.482	−.093	.614	.445
	P	.576	.576	.214	.762	.004*	.049*
	corr *P*	.7776	.804	.3945	.857	.0231**	.15876
AD_CST	*r*	.451	.65	.512	.297	.733	.653
	P	.001*	.058	.73	.325	.0001*	.002*
	corr *P*	.010**	.181	.882	.526	.002**	.0162**
FA_STR	*r*	.583	.6	.681	.972	−.048	−.118
	P	.099	.088	.010*	.11	.84	.62
	corr *P*	.229	.223	.050**	.241	.884	.81
MD_STR	*r*	.2	.844	−.055	.516	.722	.563
	P	.606	.004*	.859	.071	.0001*	.010*
	corr *P*	.805	.025**	.892	.198	.004**	.0476**
RD_STR	*r*	−.1	−.067	−.385	.407	.615	.389
	P	.798	.865	.194	.168	.004*	.09*
	corr *P*	.873	.887	.39285	.349	.027**	.221
AD_STR	*r*	.75	.117	.379	.525	.795	.451
	P	.020*	.765	.201	.065	.00001*	.046*
	corr *P*	.085**	.849	.388	.195	.00081**	.155
FA_DRTT	*r*	.683	−.15	.681	.324	.301	.061
	P	.042*	.7	.010*	.28	.198	.803
	corr *P*	.162	.886	.045**	.463	.391	.867
MD_DRTT	*r*	.3	−.133	.358	.203	.373	.075
	P	.433	.732	230	.505	.105	.759
	corr *P*	.688	.872	.405	.718	.236	.866
RD_DRTT	*r*	−.167	−.217	−.11	−.214	.075	.077
	P	.668	.576	.721	482	.753	.753
	corr *P*	.859	.791	.885	.697	.884	.871
AD_DRTT	*r*	.633	−.083	.709	.423	478	.035
	P	.067	.831	.007*	.15	.033*	.887
	corr *P*	.194	.886	.038**	.320	.134	.898

*P value less than .05.
**FDR of .10.
AD = axial diffusivity; corr P = corrected P; CST = corticospinal tract; DRTT = Dentatorubro thalamic tract; FA = fractional anisotropy; iNPH = idiopathic normal pressure hydrocephalus; MD = mean diffusivity; RD = radial diffusivity; STR = superior thalamic radiation.

driven by the sylvian sulcal CSF volume as it was statistically significantly higher in the iNPH group compared to the AD group. This finding is in line with the previous observation of the DESH sign, enlarged sylvian fissure, and tight high convexities.[5]

Follow-up quantitative sulcal CSF distribution studies on a larger scale might prove this technique to be promising in quantifying and detecting subtle changes in early stages of iNPH, particularly with the rising evidence of MRI changes years before the onset of iNPH symptoms.[21] While the total sCSFV of iNPH was comparable and not significantly different from the sCSFV in Alzheimer's and age-matched HE across lifespan. The vCSFVs of iNPH were significantly greater than AD and age-matched control. If the ventriculomegaly was due to a neurodegenerative disease, such as dementia, we would expect cortical atrophy and, therefore, increase in the sulcal CSF volume to be proportionate to the ventriculomegaly. Interestingly, however, the sulcal CSF volume of the iNPH patients was comparable to the AD and the HE. This provides a noninvasive radiological method to evaluate ventriculomegaly, an increase VV that is disproportionate to the cerebral cortical atrophy. In this study, we found the vCSF/sCSF ratio to be significantly higher in the iNPH patients when compared to AD and HE. In our study, the colossal angle less than or equal to 90° and effacement of the sulci at the brain vertex along with disproportionate ventriculomegaly in respect to the brain parenchymal volume loss were predictive of the NPH in more than 70% of the time when blinded reviewers were exposed to the mix of the AD, NPH, and HE subjects. Adding the described noninvasive imaging biomarkers will increase the PPV to above 95%. However, this needs to be further evaluated by larger number of subjects in the future studies.

The effect of iNPH on many WM tracts have been previously explored using variety of DTI techniques. Increased MDs in the periventricular WM have been reported using voxel-based analysis,[27] tract-based spatial statistics (TBSS),[28,29] and ROI analysis.[30,31] This increase in the MDs may increased diffusion of extracellular water molecules in the major projection bundles near the ventricular system in with iNPH.[32]

iNPH effect on FA value of surrounding WM pathways is more heterogeneous across the studies. Reduced FA in the

Table 3. Ventricular/Sulcal CSF Ratio in Alzheimer's Disease, Healthy Controls, and iNPH Patients

	MeanvCSFVp and SD	Mean sCSFVp and SD	vCSF/sCSF	Mean Sylvian CSFVp and SD	Mean sCSFV Minus Sylvian CSF and SD
iNPH	.078 (.023)	.073 (.012)	1.07	.014 (.004)	.059 (.01)
Alzheimer's	.031 (.01)	.076 (.007)	.40	.011 (.001)	.065 (.007)
Healthy Elderly	.01 (.004)	.058 (.0105)	.20	.008 (.0017)	.05 (.01)

CSF = cerebrospinal fluid; iNPH = idiopathic normal pressure hydrocephalus; sCSFVp = sulcal cerebrospinal fluid volume percentage adjusted to intracranial volume; SD = Standard deviation; vCSFVp = ventricular cerebrospinal fluid volume percentage adjusted to intracranial volume.

centrum semiovale and increased in the internal capsule was reported in one study using TBSS.[28] ROI-based analyses showed that FA values of the CST were increased in iNPH patients compared to healthy controls in one study[30] and decreased in another compared to normal controls and Parkinson's disease patients.[31,33] It was proposed that the increased FA value of the CST is mainly due to increase in axial diffusivity and hypothesized that the stretching and compression effect of the enlarging ventricles leads to reduced tortuosity and increased coherence of the WM tracts leads to increased diffusivity of water parallel to these fibers.[28] Additionally, axonal damage and degeneration of the crossing fibers were thought to be playing an additional role in the increased FA values in the CST. Recently, Kamiya and coauthors studied postsurgical shunting axonal stretching and recovery of the CST using multishell and higher *b* factor DWI using the neurite orientation dispersion and density imaging model and WM tract integrity, and found that the orientational coherence within the CST was higher in patients compared to controls, and some normalization happened after the shunt surgery in patients.[34]

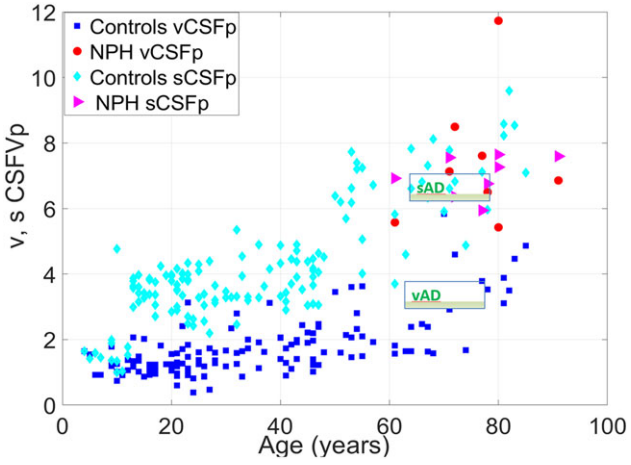

Fig 5. Idiopathic normal pressure hydrocephalus (iNPH), Alzheimer's disease, and healthy subjects' ventricular and sulcal cerebrospinal fluid (CSF) volumes: In the healthy subjects (shades of blue) and the Alzheimer's disease group (light green), the sulcal CSF volume (light blue diamond) is higher than the ventricular CSF volume (dark blue square) across lifespan and increases with age, including the age-matched healthy elderly portion. The iNPH ventricular CSF volume (red circle) is significantly higher than the other two groups. There is no difference between the iNPH sulcal CSF volume (pink triangles) and control sulcal CSF volume (light blue diamond). In the iNPH group, the CSF volume (red circles) and sulcal CSF volume (pink triangle) were not significantly different.
sAD = sulcal CSF in Alzheimer's disease; Scsfv = sulcal cerebrospinal fluid volume; sCSFVp = sulcal cerebrospinal fluid volume percentage adjusted to the intracerebral volume; vAD = ventricular CSF volume in Alzheimer's disease; vCSFV = ventricular cerebrospinal fluid volume; vCSFVp = ventricular cerebrospinal fluid volume percentage of the intracerebral volume.

It is unclear why there is asymmetry between the right and left sides in our iNPH cohort. On visual inspections of ventriculomegaly on axial imaging (see Fig 3), 3 patients had larger left lateral ventricles. This could be due to our small sample size and will need testing in larger studies. Additionally, our data does not explain why patients were present with different phenotypes. But, one could speculate that from the clinical standpoint, patients who have cognitive and gait abnormalities might have slightly different disease process than the ones who have urinary incontinence and gait abnormalities.

Limitations

Our study is limited by the small sample size and the use of different MRI protocols for iNPH, AD, and healthy subjects. We did not compare the differences in DTI-derived scalar measures of the periventricular WM tracts among the three groups as DTI data were acquired using different protocols and more studies are needed under unified MRI protocols. No quantitative assessment of test-retest reliability for the fiber tracking of WM tracts was performed, DTI quality assurance was evaluated by inspecting regional FA and MD histograms as discussed in the Methods section. We avoided FA interpretation as differences might reflect nonspecific multidirectional changes in water diffusivity secondary to the different MRI protocols. The unidirectional measures of axial, radial, and the MD are considered to be more comparable across different MRI protocols.[35] Further larger scale studies using larger sample size and unified MRI protocols are needed.

References

1. Staffaroni A, Elahi FM, McDermott D, et al. Neuroimaging in dementia. Semin Neurol 2017;37:510-37.
2. Mori E, Ishikawa M, Kato T, et al. Guidelines for management of idiopathic normal pressure hydrocephalus: second edition. Neurol Med Chir 2012;52:775-809.
3. Hakim S, Adams RD. The special clinical problem of symptomatic hydrocephalus with normal cerebrospinal fluid pressure observations on cerebrospinal fluid hydrodynamics. J Neurol Sci 1965;2:307-27.
4. Relkin N, Marmarou A, Klinge P, Bergsneider M, Black PM. Diagnosing idiopathic normal-pressure hydrocephalus: INPH Guidelines, part II. Neurosurgery 2005;57:4-16.
5. Hashimoto M, Ishikawa M, Mori E, Kuwana N. Study of INPH on neurological improvement (SINPHONI). Diagnosis of idiopathic normal pressure hydrocephalus is supported by MRI-based scheme: a prospective cohort study. Cerebrospinal Fluid Res 2010;7:18. https://doi.org/10.1186/1743-8454-7-18
6. Cabrala D, Beachb TG, Veddersa L. Frequency of Alzheimer's disease pathology at autopsy in patients with clinical normal pressure hydrocephalus. Alzheimers Dement 2012;7:509-13.

7. Pomeraniec IJ, Bond AE, Lopes MB, Jane JA. Concurrent Alzheimer's pathology in patients with clinical normal pressure hydrocephalus: correlation of high-volume lumbar puncture results, cortical brain biopsies, and outcomes. J Neurosurg 2016;124: 382-8.
8. Silverberg GD, Huhn S, Jaffe RA, et al. Downregulation of cerebrospinal fluid production in patients with chronic hydrocephalus. J Neurosurg 2002;97:1271-5.
9. Silverberg GD, Mayo M, Saul T, Rubenstein E, McGuire D. Alzheimer's disease, normal-pressure hydrocephalus, and senescent changes in CSF circulatory physiology: a hypothesis. Lancet Neurol 2003;2:506-11.
10. Eide P, Ringstad G. Delayed clearance of cerebrospinal fluid tracer from entorhinal cortex in idiopathic normal pressure hydrocephalus: a glymphatic magnetic resonance imaging study. J. Cereb. Blood Flow Metab 2018. https://doi.org/10.1177/0271678X18760974 [Epub ahead of print].
11. Ringstad G, Vatnehol, SA, Eide PK. Glymphatic MRI in idiopathic normal pressure hydrocephalus. Brain 2017;140: 2691-705.
12. Bradley WG. CSF Flow in the brain in the context of normal pressure hydrocephalus. AJNR Am J Neuroradiol 2015;36:831-8.
13. Acosta-Cabronero J, Nestor PJ. Diffusion tensor imaging in Alzheimer's disease: insights into the limbic-diencephalic network and methodological considerations. Front Aging Neurosci 2014;6:266. https://doi.org/10.3389/fnagi.2014.00266
14. Nestor SM, Rupsingh R Borrie B, Borrie M, et al. Ventricular enlargement as a possible measure of Alzheimer's disease progression validated using the Alzheimer's disease neuroimaging initiative database. Brain 2008;131:2443-54.
15. Osuka S, Matsuhita A, Yamamoto T, et al. Evaluation of ventriculomegaly using diffusion tensor imaging: correlation with chronic hydrocephalus and atrophy. J Neurosurg 2010;112:832-9.
16. Hoza D, Vlasák A, Hořínek D, et al. DTI-MRI biomarkers in the search for normal pressure hydrocephalus aetiology: a review. Neurosurg Rev 2015;38:239-44.
17. Siasios I, Kapsalaki EZ, Fountas KN, et al. The role of diffusion tensor imaging and fractional anisotropy in the evaluation of patients with idiopathic normal pressure hydrocephalus: a literature review. Neurosurg Focus 2016;41:12. https://doi.org/10.3171/2016.6.FOCUS16192
18. Keser Z, Hasan KM, Mwangi BI, et al. Diffusion tensor imaging of the human cerebellar pathways and their interplay with cerebral macrostructure. Front Neuroanat 2015;9:1-13.
19. Tsunoda A, Mitsuoka H, Sato K, Kanayama S. A quantitative index of intracranial cerebrospinal fluid distribution in NPH. Neuroradiology 2000;42:424-9.
20. Williams MS, Relkin N. Diagnosis and management of idiopathic normal-pressure hydrocephalus. Neurol Clin Pract 2013;3: 375-85.
21. Engel DC, Adib SD, Schuhmann MU, Brendle C. Paradigm-shift: radiological changes in the asymptomatic iNPH-patient to be: an observational study. Fluids Barriers CNS 2018;15:1-7.
22. Hasan KM, Walimuni IS, Abid H, Hahn KR. A review of diffusion tensor magnetic resonance imaging computational methods and software tools. Comput Biol Med 2011;41:1062-72.
23. Benjamini Y, Hochberg Y. Controlling the false discovery rate: a practical and powerful approach to multiple testing. J R Statist Soc B. 1995;57:289-300.
24. Mori S, Wu D, Ceritoglu C, et al. MRICloud: delivering high-throughput MRI neuroinformatics as cloud-based software as a service. Comput Sci Engin 2016;18:21-35.
25. Wakana S, Caprihan A, Panzenboeck MM, et al. Reproducibility of quantitative tractography methods applied to cerebral white matter. Neuroimage 2007;36:630-44.
26. Haines DE. *Neuroanatomy: an atlas of structures, sections, and systems 8th edition.* Baltimore, MD: Williams & Wilkins; 2008:178-87.
27. Kanno, S, Abe N, Saito M, Takagi M, Nishio Y. White matter involvement in idiopathic normal pressure hydrocephalus: a voxel-based diffusion tensor imaging study. J Neurol 2011;258: 1949-57.
28. Hattori T, Yuasa T, Aoki S, et al. Altered microstructure in corticospinal tract in idiopathic normal pressure hydrocephalus: comparison with Alzheimer disease and Parkinson disease with dementia. AJNR Am J Neuroradiol 2011;32:1681-7.
29. Reiss-zimmermann M, Scheel M, Dengl M, Preuß M, Fritzsch D, Hoffmann K. The influence of lumbar spinal drainage on diffusion parameters in patients with suspected normal pressure hydrocephalus using 3T MRI. Acta Radiol 2014;55:622-30.
30. Hattingen E, Jurcoane A, Melber J, et al. Diffusion tensor imaging in patients adult chronic idiopathic hydrocephalus. Neurosurgery 2010;66:917-24.
31. Keong NC, Pena A, Price SJ, et al. Diffusion tensor imaging profiles reveal specific neural tract distortion in normal pressure hydrocephalus. PloS One 2017;12:1-25.
32. Aygok G, Marmarou A, Fatouros P, Young H. Brain tissue water content in patients with idiopathic normal pressure hydrocephalus. Acta Neurochir 2006;96:348-51.
33. Marumoto K, Koyama T, Hosomi M, et al. Diffusion tensor imaging in elderly patients with idiopathic normal pressure hydrocephalus or Parkinson's disease: diagnosis of gait abnormalities. Fluids Barriers CNS 2012;9:20. https://doi.org/10.1186/2045-8118-9-20
34. Kamiya K, Hori M, Irie R, et al. Diffusion imaging of reversible and irreversible microstructural changes within the corticospinal tract in idiopathic normal pressure hydrocephalus. NeuroImage Clin 2017;14:663-71.
35. Huang H, Zhang J, van Zijl PC, Mori S. Analysis of noise effects on DTI-based tractography using the brute-force and multi-ROI approach. Magn Reson Med 2004;52:559-65.